Design of multi-spectrum BRDF measurement system

Zhongyi Zhao (赵忠义), Chao Qi (齐 超), and Jingmin Dai (戴景民)

Department of Automatic Measurement and Control, Harbin Institute of Technology, Harbin 150001

Received March 27, 2006

A multi-spectrum bidirectional reflectance distribution function (BRDF) measurement system was developed with the adoption of single reference standard measurement method. An arm-adjustable corner device was designed for the BRDF system. Changing the distance to the sample by moving the detector arm made the device applicable to different wavelengths. The system could be used for the spectrum range from visible light (0.6328 μm) to mid-far infrared (10.6 μm), the facular size between 0.8—3 cm. The rotating limit of detector arm was $\pm 180^\circ$, the rotation range of sample holding table was 360°, and the angle resolution was 0.036°. A silicon carbide sample was measured using this system with reflectance zenith from -55° to $+55^\circ$. According to the error analysis, the measurement uncertainty of this device was about 6.42%.

OCIS codes: 120.5820, 220.4830, 290.5820, 070.1170.

Bidirectional reflectance distribution function (BRDF) is a fundamental quantity that describes the reflectance properties of samples in such different applications as remote sensing, computer graphics, and image interpretation. It shows the pattern of light reflected from a surface of the material into all directions above the surface when an incident light comes from a particular direction. For an isotropic surface, the BRDF determines the appearance of material from different view directions. Since the actual BRDF is a complicated multi-dimensional function, the simplified models known as the diffuse reflectance and specular reflectance are often used to describe the complete reflectance.

Measuring BRDF is the most direct way to acquire the surface reflectance characteristics of target materials, and many kinds of materials are measurable. Different kinds of models should be used to simulate the reflectance characteristics of different material surfaces whereas the modeling describing the reflectance characteristics of material surface depends directly on the effective BRDF measurement. The instrument to measure BRDF is normally named as bidirectional reflectometer or scatterometer, and its components include a light source, a manual or automatic goniometer, one or a set of detectors, and a suit of data collection system.

Currently, BRDF measurements are mainly performed by changing the relative positions between the detector, sample, and light source to realize the direction changes of incidence and reflectance within the space[1−5]. Zhang *et al.* used the design of fixed detector and rotating sample and light source to measure the BRDF[5]. The scheme will be comparatively simple if we have no strict requirements on the corner precision; but multiple corner tables and shift tables should be used for some special purposes. In addition, goniometer table will be placed in vacuum environment in some devices. In order to realize rapid sampling and improve the sensitivity, multiple detectors or optical fibers would be used.

The traditional BRDF measurement instrument is quite expensive and is complicated to operate with long measuring time, which goes against its application in practice. Thereby, it is exigent to develop a simple, rapid, and low cost instrument with good precision. This measurement should be able to measure reflectance not only for flat samples but also for curve materials. Since it is difficult to capture the light with too long or too short wavelength, the measuring range of most instruments is from visible light to near infrared (NIR).

The BRDF is defined as the ratio of the radiance scattered by a surface into the direction to the collimated irradiance incident on a unit area of the surface[6]

$$f_{\rm r}(\theta_{\rm i},\varphi_{\rm i};\theta_{\rm r},\varphi_{\rm r}) = \frac{{\rm d}L_{\rm r}(\theta_{\rm i},\varphi_{\rm i};\theta_{\rm r},\varphi_{\rm r})}{{\rm d}E_{\rm i}(\theta_{\rm i},\varphi_{\rm i})} = \frac{{\rm d}L_{\rm r}(\theta_{\rm i},\varphi_{\rm i};\theta_{\rm r},\varphi_{\rm r})}{{\rm d}L_{\rm i}(\theta_{\rm i},\varphi_{\rm i})\cos\theta_{\rm i}{\rm d}\omega_{\rm i}}, \quad (1)$$

where θ is the zenith angle and ϕ is the azimuth angle under standard spherical coordinates, the subscripts "i" and "r" denote the incident and scattered quantum respectively, ${\rm d}L_{\rm r}(\theta_{\rm i},\varphi_{\rm i};\theta_{\rm r},\varphi_{\rm r})$ is the reflectance irradiance in the direction of $(\theta_{\rm r},\varphi_{\rm r})$, ${\rm d}E_{\rm i}(\theta_{\rm i},\varphi_{\rm i})$ is the incident irradiance in the direction of $(\theta_{\rm i},\varphi_{\rm i})$, ${\rm d}L_{\rm i}(\theta_{\rm i},\varphi_{\rm i})$ is the incident radiance in the direction of $(\theta_{\rm i},\varphi_{\rm i})$, ${\rm d}\omega_{\rm i}$ is the radiation solid angle in the direction of $(\theta_{\rm i},\varphi_{\rm i})$. It is obvious that BRDF is a four angle variable, and it depends also on the temperature and roughness of material surface.

BRDF measurement includes absolute and relative measurements. Absolute measurement is done without any reference standards; relative measurement is a comparison between the sample and the reference standard with known reflectance. The latter is a commonly used method to measure BRDF, and it can be further divided as substitution measurement and single-reference measurement. Theoretically, relative measurement is two measurements on reference standard and sample at each orientation with different incident angles. But in practice, the point-to-point measurement to the reference standard is seldom used. Instead, single-reference measurement is commonly adopted.

We used the single-reference measurement which could restrain the stray light caused by the environment and the parts by apparatus[7] in the system. The BRDF

measurement system consists of four major components: a light source, a corner device, a detector and data acquisition and processing system. With the laser fixed, the relative changes of incident direction and reflectance receiving direction within the hemisphere space could be realized by rotating the sample within the surface and by changing position of the detector.

The used light sources and the corresponding photoelectric detectors are listed in Table 1. The spectrum range of our designed BRDF measurement system is from visible light (0.6328 μm) to NIR (1.34 μm) to middle infrared (IR) (3.39 μm) until mid-far IR (10.6 μm). Radiation emitted from laser is consolidated to a beam of 20-mm diameter by each expander collimation system. The beam firstly passes through an attenuator, undrawn by an off-axis parabolic mirror, and then passes successively through the aperture stop, the pinhole, and the in-phase chopper, finally it is focused by a spherical lens to the sample. The focal spot is close to Airy disc with the diameter of 1—3 cm.

Figure 1 shows the BRDF measurement system. The sample is placed on the corner device piloted by three motors. The computer precisely controls the motor corner by a numerical servo motor card 6020. This corner device consists of two groups of modules: the sample rotating module (motor A, sample rotating table, and dial A) and the detector rotating module (motor B, motor C, detecting arm, and dial B). So the detector could move along horizontal and vertical directions. The sample is placed on the experimental table which has three degrees of freedom, and it rotates within the range from $-90°$ to $+90°$ with the force of motor A to control the change of incident angle. The sample's rotating angle could be numerated by the dial A. Motor B's axis is in parallel with the table-board and in vertical with the plane normal. Motor B drives the detector arm to rotate within the range from $-180°$ to $+180°$, while its axis is in the same level with the sample center. Utilizing the gear deceleration configuration, motor C drives the detector arm to rotate around the center axis within the range from $-180°$ to $+180°$. The rotate angles of sample and detector arm are indicated respectively by dial A and dial B. With the combination of the above three motors, the change of zenith $\theta_{\rm i}$ and azimuth $\varphi_{\rm i}$ incident on the sample could be realized. In this way, the scattered irradiance from the sample could be measured as the function of spatial reflected angle $(\theta_{\rm r}, \varphi_{\rm r})$.

Table 1. Lasers and Detectors Used in the BRDF Measurement System

Laser	Wavelength (μm)	Beam Diameter (mm)	Photoelectric Detector
He-Ne	0.6328	1.5	Si1336-5BK
YVO_4	1.34	2.0	PbS325g-02
He-Ne	3.39	1.0	PbS325g-02
CO_2	10.6	2.0	HgCdTe (77 K)

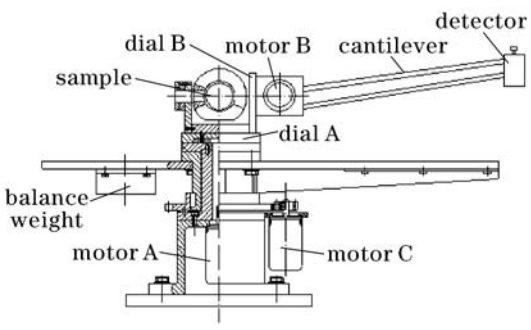

Fig. 1. BRDF measurement system.

The BRDF depends on four angles and it needs strict precision of corner device. So we selected Panasonic MSMA5AZA step motor. By using the closed loop control of universal impulse negative feedback response for motor displacement, we can obtain more accurate displacement control and more stable motor rev. The motors are controlled directly by the drivers. Software programming determines clockwise or anti-clockwise rotation angle to change the relative positions between sample azimuth, incident light, and photoelectric detector.

Different from other corner devices in BRDF measurement system, we designed a double-poles detector cantilever structure. Adjusting the slide block on the detector arm could make the device applicable to BRDF measurement for different wavelengths. The rotation of the sample and the detector arm could realize the relative movement between the sample and detector to fulfill the measurements of the reflectance characteristics, scattering characteristics, and spectrum characteristics in the hemisphere space.

The light scattered from the sample under different wavelengths is received by the corresponding photoelectric detector, then enters through the preamplifier into the signal input stop of lock-in amplifier. The reference signal of lock-in amplifier is provided by the chopper. The lock-in amplifier outputs direct current (DC) voltage signals which are received by multi-port simulated data acquisition module Nu DAM-6107, then the signals pass through RS485-RS232 organic transform module ND-6520 into the data processing system.

Experiment procedure contains the acquisition of raw BRDF data and data processing. Silicon carbide has the virtues of proportional crystal grain size and wearable surface. The light sources used are a He-Ne laser with the wavelength of 0.6328 μm and power of 8 mW and a YVO_4 laser with the wavelength of 1.34 μm and current of 0.6 A. Taking 1500CCR/RC.S.G waterproof grinding silicon carbide as target, we performed the measurement under positive direction with the reflectance zenith angle from $-55°$ to $+55°$. The obtained data are shown in Tables 2 and 3.

From Tables 2 and 3 we can see that the reflectance near the positive incident light is a little stronger, and the values are reduced with the augmentation of reflectance zenith angle. Silicon carbon shows a reflectance close to a Lambert diffuse cosine when the forward and backward reflectance zenith angle is less than 60°. This basically matches the result obtained by Dereniak *et al.*[8].

Our BRDF measurement system thoroughly considered a series of important random errors coming from circuitry detector response, calibration of the goniometer, environment temperature, and artificial reading etc..

Table 2. Experimental Results at 0.6328-μm Wavelength Using Si Detector

θ_s (deg.)	-15	-25	-35	-45	-55	55	45	35	25	15
V (mV)	175 ± 5	170 ± 15	160 ± 10	153 ± 9	142 ± 5	160 ± 10	166 ± 10	160 ± 15	170 ± 15	180 ± 10

Table 3. Experimental Results at 1.34-μm Wavelength Using PbS Detector

θ_s (deg.)	-20	-30	-40	-50	55	45	35	25
V (mV)	1272 ± 5	1268 ± 2	1270 ± 3	1265 ± 3	1260 ± 6	1263 ± 2	1262 ± 2	1265 ± 5

The BRDF measurement uncertainty, $\varepsilon_{\mathrm{BRDF}}$, can be evaluated and expressed by[9]

$$(\varepsilon_{\mathrm{BRDF}})^2 = 2(\varepsilon_{\mathrm{NS}})^2 + 2(\varepsilon_{\mathrm{LIN}})^2 + (\varepsilon_{\mathrm{SLD}})^2 + (\varepsilon_{\theta_s} \tan\theta_s)^2, \quad (2)$$

where $\varepsilon_{\mathrm{NS}}$ is the noise-to-signal ratio error, $\varepsilon_{\mathrm{LIN}}$ represents the nonlinearity error of the electronics, $\varepsilon_{\mathrm{SLD}}$ is the error of the receiver solid angle (view angle), ε_{θ_s} is the error of the total scattering zenith angle, and θ_s is the receiver scattering zenith angle. The error of the receiver solid angle $\varepsilon_{\mathrm{SLD}}$ is

$$(\varepsilon_{\mathrm{SLD}})^2 = (2\varepsilon_{\mathrm{RM}})^2 + (2\varepsilon_{\mathrm{R}z})^2 + (2\varepsilon_{\mathrm{RA}})^2, \quad (3)$$

where $\varepsilon_{\mathrm{RM}}$ is the error in the goniometer receiver arm radius, $\varepsilon_{\mathrm{R}z}$ is the error of the receiver arm radius due to sample z-direction misalignment, and $\varepsilon_{\mathrm{RA}}$ is the error of the receiver aperture radius. The total scattering zenith angle error, ε_{θ_s}, is given by

$$(\varepsilon_{\theta_s})^2 = (\varepsilon_{\theta\mathrm{M}})^2 + (\varepsilon_{\theta z})^2 + (\varepsilon_{\theta\mathrm{T}})^2, \quad (4)$$

where $\varepsilon_{\theta\mathrm{M}}$ is the error of the goniometer scattering angle, $\varepsilon_{\theta z}$ is the error due to sample z-direction misalignment, and $\varepsilon_{\theta\mathrm{T}}$ is the sample tilt error.

Based on the developed full-automation BRDF measurement system and the practice measurement, the error expression could be expanded as

$$(\varepsilon_{\mathrm{BRDF}})^2 = 2(\varepsilon_{\mathrm{NS}})^2 + 2(\varepsilon_{\mathrm{LIN}})^2 + (\varepsilon_{\mathrm{SLD}})^2 + (\varepsilon_{\theta_s} \tan\theta_s)^2 + \varepsilon_\lambda^2 + \varepsilon_t^2 + \varepsilon_0^2, \quad (5)$$

where the three accessorial items ε_λ, ε_t, ε_0 are respectively the light source error, environment temperature error, and artificial reading error.

Each of the above errors was measured independently. The error due to the noise-to-signal ratio $\varepsilon_{\mathrm{NS}}$ could be obtained by the noise detector. To each measuring point about every 2 s, its minimum value is 0.1%. Therefore, $\varepsilon_{\mathrm{NS}}$ equals 0.001 for both incident power measurement and scattering power measurement.

Nonlinearity error $\varepsilon_{\mathrm{LIN}}$ of detector and circuitry mainly comes from detector array noise, null shift, low frequency current noise of transistor in the preamplifier, nonlinearity distortion caused by the overload of lock-in amplifier and so on. Photoelectric signal is received by detector firstly and then passes through preamplifier, lock-in amplifier and then to output; the electric error is up to 0.35%.

The receiver solid angle error $\varepsilon_{\mathrm{SLD}}$ is caused by three factors. The first is due to the error in the goinometer's receiver arm radius. The detector cantilever is 700 mm in length, and the mechanical processing error is 0.3 mm. The second stems from errors in the sample z-direction misalignment. The sample z error is made up of the goniometer error and the user alignment error. The theodolite measurement shows that the goniometer z error is 0.15 mm. If the errors during alignment of the sample are same, then a total root mean square (RMS) z error of 0.2 mm is used in the error analysis. The last component of the solid angle error comes from the size of the receiver's aperture. By careful design of the electro-optical system of the receiver, we can make the mechanical aperture be the actual aperture. The aperture error is 0.15%. So according to Eq. (3), $\varepsilon_{\mathrm{SLD}}$ is about 0.7%.

Scattering zenith angle error ε_{θ_s} is based on the angle error of the system, it can be taken as 0.072° equally within a circle caused by the rotation of the motor; the error caused by sample z-direction misalignment is around 1°. Then according to Eq. (4), ε_{θ_s} is 0.28%.

Since we use single-reference measurement, light source error of the system is very small. But considering the power random vibration and temperature drift of the laser beam during the replacement of reference standard and sample, we take ε_λ as 0.2%. Environment temperature is 25 °C, temperature precision is ±0.1 °C, and then ε_t is 0.4%. Artificial reading error is caused by different readers, according to several samples' actual measurement, ε_0 is 6.34%.

Taking above results into Eq. (5), then

$$\varepsilon = \sqrt{2\varepsilon_{\mathrm{NS}}^2 + 2\varepsilon_{\mathrm{LIN}}^2 + \varepsilon_{\mathrm{SLD}}^2 + \varepsilon_{\theta_r}^2 + \varepsilon_\lambda^2 + \varepsilon_t^2 + \varepsilon_0^2} \approx 6.42\%. \quad (6)$$

Because of the existence of light source minor vibration, detector and circuit noise interference, instrument mechanical processing precision, temperature changing, background stray-disperse radiation, and the manual random error, it is not an easy task to measure the BRDF of the sample precisely and accurately. At the same time, due to some unpredictable reasons, the actual BRDF precision is not so high.

In conclusion, an instrument to measure the space reflectance characteristics of material surface is developed. The measured spectrum ranges from 0.6328 μm of visible light to 10.6 μm of mid-far IR. The reflectance characteristic measurement is realized. The uncertainty of BRDF system is 6.42%.

This work was supported by the Key Subject Fund of 985II, the Postdoctoral Fund of China, and the Postdoctoral Fund of Heilongjiang Province (No. 20060390783).
Z. Zhao's e-mail address is zhongyi_zhao@hit.edu.cn.

References

1. K. J. Dana, in *Proceedings of 8th IEEE International Conference on Computer Vision* **2,** 460 (2001).
2. S. Tsuchida, I. Sato, and S. Okada, Proc. SPIE **3870,** 254 (1999).
3. S. R. Marschner, S. H. Westin, E. P. F. Lafortune, K. E. Torrance, and D. P. Greenberg, in *Proceedings of 10th Eurographics Workshop on Rendering* 139 (1999).
4. J. R. Johnson, W. M. Grundy, and M. K. Shepard, Icarus **171,** 546 (2004).
5. B. Zhang, W. Liu, Q. Wei, M. Gao, C. Lian, J. Hu, and S. Wang, Opt. Technique (in Chinese) **32,** 180 (2006).
6. F. E. Nicodemus, Appl. Opt. **9,** 1474 (1970).
7. C. Qi, C. Yang, W. Li, and J. Dai, Chin. Opt. Lett. **1,** 398 (2003).
8. E. L. Dereniak, T. W. Stuhlinger, and F. O. Bartell, Proc. SPIE **257,** 184 (1980).
9. T. F. Schiff, M. W. Knighton, D. J. Wilson, F. M. Cady, J. C. Stover, and J. J. Butler, Proc. SPIE **1995,** 121 (1993).